

## **LABORATORY EFFORTS TO DEVELOP A BOREHOLE NONDESTRUCTIVE TESTING SYSTEM TO INSPECT IN SITU FOUNDATION ELEMENTS**

*Alireza Kordjazi, Temple University, Philadelphia, PA*

*Joseph T. Coe, Temple University, Philadelphia, PA*

### **Abstract**

A nondestructive testing system was developed to evaluate foundations embedded in the subsurface. The system functions by generating elastic stress waves as it is lowered in a borehole alongside the foundation. Reflections from the foundation element are recorded and plotted to develop a high resolution image. The system is intended for inspection purposes of in-service foundation elements, particularly deep foundations for critical infrastructure. In this study, a large soil model was developed with a reduced-scale deep foundation element embedded within the model subsurface so that system performance could be evaluated. The foundation element features several anomalies, which replicate issues with foundation integrity in the field. The system was capable of differentiating between competent and anomalous sections of the foundation element. A summary of hardware components, system operation, and soil model construction/geometry is presented as well as the results from laboratory testing.

### **Introduction**

Proper inspection is necessary to ensure confidence in the satisfactory performance of deep foundations since construction often plays a major role in foundation behavior. Soil caving, faults in concrete placement, and corrosion are the typical causes of section loss in deep foundations (O'Neil, 1991; Brown et al., 2010). Sarhan et al. (2002) reported that even minor defects with a size of approximately 10 percent of the cross-sectional area of a drilled shaft can reduce its lateral load capacity by 11%. Moreover, knowledge of the integrity of in-service foundations, many of which are of unknown geometry, is often of paramount importance to avoid foundation failure. For example, the long term performance of in-service steel piling can be compromised due to corrosion from ground water. Since visual inspection of deep foundations is often impossible, many non-destructive tests (NDT) have been developed to evaluate foundation integrity both during construction and post-construction. Among these NDT techniques, sonic echo (SE), cross-hole sonic logging (CSL), and gamma-gamma logging (GGL) are commonly used (Finno and Gassman, 1998; Iskander et al., 2003; Jalinoos et al., 2005). Recent advances in NDT for drilled shafts have also led to the development of the thermal integrity profiling (TIP) method (Mullins, 2010). Many of the aforementioned methods suffer from a range of issues. For example, there may be limited coverage of the cross sectional area of the foundation and restriction in the timeframe of testing. Additionally, these methods are often unable to evaluate the integrity of the cover concrete outside the rebar cage that is more critical in preventing corrosion of a drilled shaft (Samtani et al., 2005). Except for some efforts that have attempted electrical resistivity measurements on concrete structures (Polder and Peelen, 2002; Morris et al., 2002), there is no specific NDT technique that has been identified with the potential to evaluate corrosion in deep foundations. This brief discussion underlines the need for other complementary NDT techniques that can address such existing limitations. The application of high frequency stress waves (Lee and Santamarina, 2005; Coe and Brandenburg, 2010) in geotechnical engineering, despite some limitations (Coe and Brandenburg, 2012), has been shown to be a promising tool that may be adaptable to address the aforementioned issues

regarding in situ evaluate of in-service foundations. This paper examines an ultrasonic borehole probe that was developed to image the outer circumference of deep foundations for the purposes of in situ foundation inspection.

## Laboratory Model and System Components

In this study, a laboratory soil model was prepared inside a large stainless steel cylindrical container with wall thickness of 0.6 cm (0.25 in), an exterior diameter of 0.6 m (2 ft), and a height of 0.9 m (3 ft). Silica sand was air-pluviated through a #16 sieve from a consistent drop height of 0.9 m (3 ft) into the container to develop a uniform soil profile. The soil model also contained two model foundation elements and a 15.2 cm (6 in) diameter PVC pipe that mimicked a borehole alongside the two foundation elements. Figure 1(a) shows the schematic of the model. Despite the use of a laboratory scale soil model, the two foundation elements represent real-scale deep foundations systems. However, only a limited length of each foundation is modeled in order to accommodate each element inside the soil chamber in the laboratory. The upper part of the model contained a 0.3 m (1 ft) long carbon steel pipe, cut in half along its length, with outer diameter of 25.4 cm (10 in) and wall thickness of 0.95 cm (0.375 in). The steel pipe was also filled with concrete as commonly encountered in practice. As shown in Figure 1(b), the pile was divided into three sections to model different effects of corrosion: (1) a length of 12.7 cm (5 in) where no corrosion was modeled to serve as a baseline; (2) a thinned section 10.2 cm (4 in) wide and 7.6 cm (3 in) in length where 0.6 cm (0.25 in) of the wall was machined off at its centerline; and (3) complete section loss over an area 10.2 cm (4 in) wide and 10.2 cm (4 in) long. The lower part of the soil model contained a 0.3 m (1 ft) long foundation element that simulated a drilled shaft [Figure 1(c)]. The drilled shaft was cast in a way that mimicked the outside section from a 0.9 m (3 ft) diameter drilled shaft. The first 10.2 cm (4 in) of vertical length along the drilled shaft was maintained to serve as a baseline for a competent drilled shaft section. A trench shaped defect was then created over the remaining length of the drilled shaft to mimic a void. This defect exposed the longitudinal and transverse reinforcing steel rebar. The longitudinal rebar also did not extend the full length of the drilled shaft to model unintended cage movement during construction.

Upon the completion of the air pluviation process for placing the sand in the model, air was pulled out of the container using a vacuum pump. CO<sub>2</sub> was then injected into the container from the bottom to expel out any remaining air. De-aired water was then introduced at a very low rate from the bottom of the container to ensure full saturation similar to conditions below the water table in field. The system used in this study was a custom prototype based on a field system originally developed to attach to a cone penetrometer (Coe and Brandenburg, 2012). The components were later modified to allow the system to be lowered into a cased borehole drilled alongside a foundation element (Coe and Kermani, 2016). The system consisted of a pair of 100 kHz P-wave transducers (Ultran Group Model GRD100-D50) enclosed within a metallic housing and corresponding data acquisition hardware (e.g., pulser, function generator, digitizer, etc.). Coe and Kermani (2016) provides a more detailed discussion of system components.

## Data Acquisition and Analysis

All data was collected using a common-offset seismic reflection approach with a 5 mm interval between shot locations. The centerline of the transducers was level with the top edge of the model container at the start of data acquisition. This resulted in a total of 143 traces along an investigation depth of 0.72 m (2.4 ft). Given the geometry of the probe housing the transducers, the bottom 0.15 m (0.5 ft) of the container was not imaged. Moreover, when the model was placed under vacuum, some

sand found its way through the bottom of the PVC pipe, leading to a corresponding reduction in the investigation depth. The acquired data was processed and analyzed using custom Matlab<sup>®</sup> scripts that applied filters and gain to the signals.

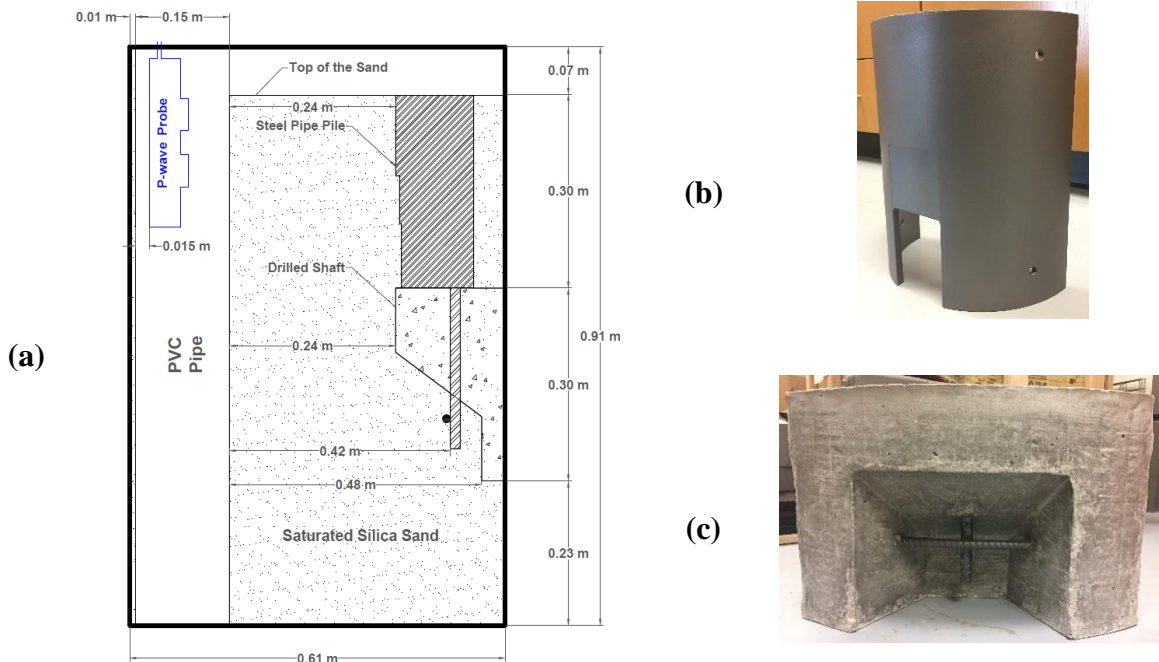


**Figure 1:** Details of the model: (a) Schematic of the model profile; (b) Steel pipe, prior to filling with concrete; (c) Drilled shaft model with the anomaly

Figure 2 plots the resulting processed reflection signals at their appropriate locations with depth. Also included in Figure 2 is an overlay of the expected model profile for comparison purposes. The reflection image clearly contains strong reflections from the foundation elements that match the expected location of the elements in the soil model and clearly distinguishes the subtle changes in the geometries. However, since each trace is normalized by its largest amplitude, the location of the longitudinal rebar is not very obvious initially in Figure 2(a). However, by narrowing the imaging window to remove very strong reflections from the shaft itself and manipulating the gain function, the location of the steel rebar is clearly illustrated in Figure 2(b). Since the effects of the PVC casing thickness and delay line were not incorporated into the estimates of the distance from the probe, the reflection signals appear to be imaged slightly closer to the probe than the constructed dimensions. However, this effect is consistent throughout the profile and it is still possible to make comparative inferences regarding changes in model geometry based on the reflection signals. For example, the steel pile baseline is definitely located closer to the transducers than the sections corresponding to defects in the pile. This difference is approximately 5 mm, which agrees reasonably well with the 6 mm difference created by machining the steel pipe. So it is possible to identify areas of corrosion on the steel pile based on the results from this preliminary laboratory study. One area of concern is the inability to accurately image the sloping section of the shaft defect. This is likely due to the strong transducer directivity pattern and the likely path of the reflection signal away from the transducers caused by the sloped section. However, despite this limitation, the reflection from the back of the void is clearly visible behind the longitudinal rebar. This demonstrates that the extent of collapse in cover concrete for a drilled shaft can be estimated using this approach even if reflection signals from the sloped sections in the collapse are not visible.

## Conclusion:

The results from this laboratory study demonstrated that high frequency ultrasonic stress waves can be used in a common offset reflection mode to successfully image defects due to corrosion in steel pipe piles and section loss in drilled shafts. The system was capable of detecting a 5 mm change in cross section for the steel pile defect and could identify the location of section loss and longitudinal rebar within the drilled shaft. Therefore, the imaging system in this study shows tremendous promise as a foundation NDT inspection technique to augment those available in the current state of the practice. Future efforts to adapt this laboratory system for field efforts should consider adopting more efficient sources of high frequency stress waves, increasing the number of stacks in data acquisition and applying more sophisticated techniques for data acquisition and analysis to improve overall system performance.

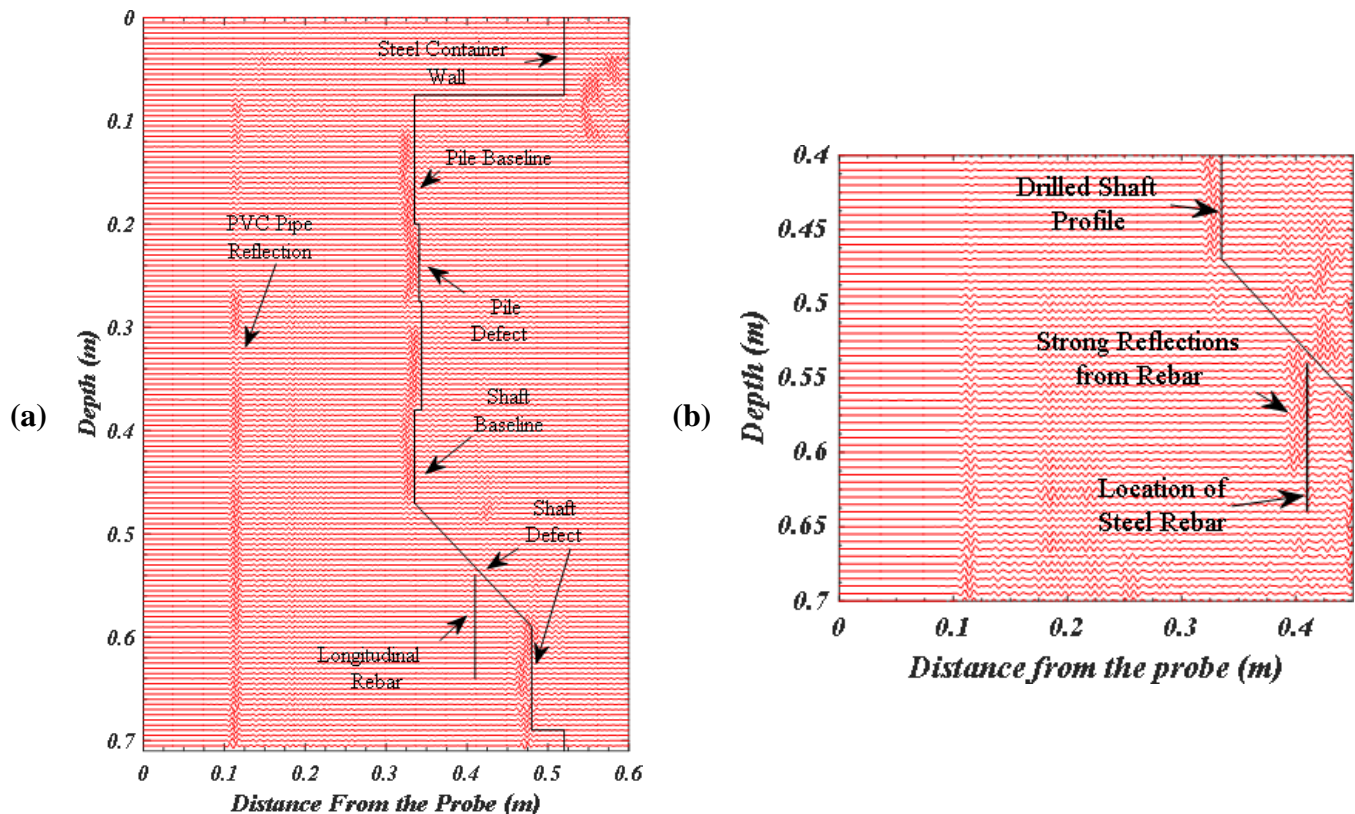


**Figure 2:** The processed traces and the expected profile of the foundation elements: (a) Entire record length; and (b) Zoomed-in to highlight the efficiency of the system in the detection of the steel rebar.

## References

- Brown, D.A., Turner, J.P., Castelli, R.J. *Drilled Shafts: Construction Procedures and LRFD Design Methods*. Publication No. FHWA-NHI-10-016, Washington, D.C., 2010, p. 970.
- Coe, J. T. and Brandenburg, S. J. "P-wave Reflection Imaging of Submerged Soil Models Using Ultrasound." *J. Geotech. Geoenviron. Eng.*, 136(10), 2010, pp. 1358-1367.
- Coe, J. T. and Brandenburg, S. J. "Cone Penetration Test-Based Ultrasonic Probe for P-wave Reflection Imaging of Embedded Objects." *J. Bridge Eng.*, 17(6), 2012, pp. 940 – 950.

- Coe, J.T., and Kermani, B. "Comparison of Borehole Ultrasound and Borehole Radar in Evaluating the Length of Two Unknown Bridge Foundations." *DFI Journal*, 10(1), 2016, pp. 8-24.
- Finno, R. and Gassman, S. "Impulse Response Evaluation of Drilled Shafts." *J. Geotech. Geoenviron. Eng.*, 124(10), 1998, pp. 965-975.
- Iskander, M., Roy, D., Kelley, S., and Ealy, C. "Drilled Shaft Defects: Detection, and Effects on Capacity in Varved Clay." *J. Geotech. Geoenviron. Eng.*, 129(12), 2003, pp. 1128-1137.
- Jalinoos, F., Mekić, N., Grimm, R.E., and Hanna, K. *Defects in Drilled Shaft Foundations: Identification, Imaging, and Characterization*. FHWA-CFL/TD-05-003, Lakewood, CO, 2005, p. 138.
- Lee, J.S. and Santamarina, C.J. "P-Wave Reflection Imaging." *Geotech. Test. J.*, 28(2), 2005, pp. 197-206.
- Morris, W., Vico, A., Vazquez, M., and De Sánchez, S.R. "Corrosion of reinforcing steel evaluated by means of concrete resistivity measurements." *Corrosion Science*, 44(1), 2002, pp. 81-99.
- Mullins, G. "Thermal integrity profiling of drilled shafts." *DFI Journal*, 4(2), 2010, pp. 54-64.
- O'Neil, M.W. "Construction Practices and Defects in Drilled Shafts." *Transportation Research Record*, 1331, 1991, pp. 6 – 4.
- Polder, R.B., and Peelen, W.H.A. "Characterisation of chloride transport and reinforcement corrosion in concrete under cyclic wetting and drying by electrical resistivity." *Cement and Concrete Composites*, 24(5), 2002, pp. 427-435.
- Sarhan, H.A., O'Neil, M.W., and Hassan, K.M. "Flexural Performance of Drilled Shafts with Minor Flaws in Stiff Clay." *J. Geotech. & GeoEnviron. Eng.*, 128(12), 2002, pp. 974 – 985.
- Samtani, N.C., Jalinoos, F., and Poland, D.M. "Integrity Testing of Drilled Shafts - Existing and New Techniques." *Proc. GEO Construction Quality Assurance/Quality Control Conference*, ADSC: the International Association of Foundation Drilling, Dallas, TX, 2005, pp. 596 – 608.